Unified equations of state for neutron stars

Nicolas Chamel
Institute of Astronomy and Astrophysics
Université Libre de Bruxelles, Belgium

in collaboration with
J. M. Pearson (UMontréal), S. Goriely (ULB), A. F. Fantina (GANIL),
A. Potekhin (Ioffe), F. Gulminelli (LPC), L. Perot (ULB), C. Ducoin (IPNL),
J.-L. Zdunik (CAMK), P. Haensel (CAMK)
Zh. Stoyanov (Sofia), Y. Mutafchieva (Sofia)
Live-Palm Kubushishi (ULB)

IAA bruxelles
ULB
fnrs LA LIBERTÉ DE CHERCHER

GdR RESANET/OG

Challenge

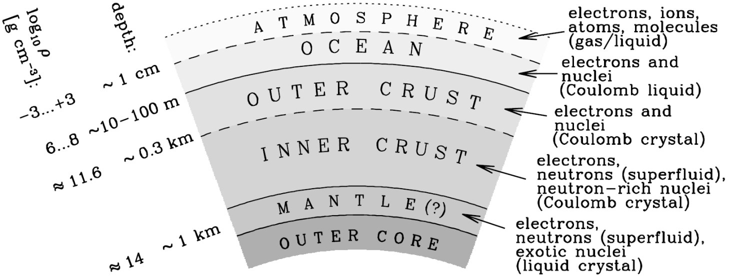

Haensel, Potekhin, Yakovlev, "Neutron Stars" (Springer, 2007)

The interior of a neutron star exhibits

- very **different phases** (gas, liquid, solid, superfluid, etc.)
- over a very **wide range of densities**
- with possibly exotic particles (hyperons, quarks) in the inner core.

Blaschke&Chamel, Astrophys. Space Sci. Lib. 457, eds L. Rezzolla, P. Pizzochero, D. I. Jones, N. Rea, I. Vidaña p. 337-400 (Springer, 2018), arXiv:1803.01836

Need for a unified treatment

- **Ad hoc matching** of different models of dense matter can lead to significant errors on the neutron-star structure & dynamics.

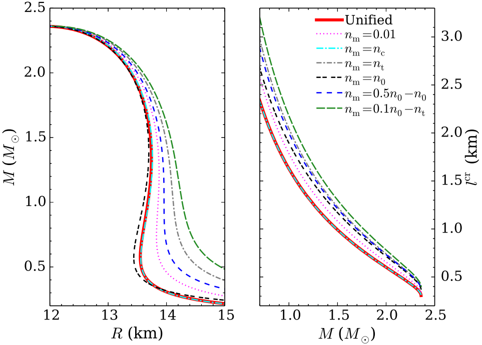

Fortin et al., Phys.Rev.C94, 035804 (2016)

- Combining inconsistent microscopic inputs leads to **multiple interpretations** of astrophysical phenomena (degeneracy).

This calls for a unified description of neutron-star interiors.

Outline

1. Internal constitution of a neutron star
   - Unified description
   - Constraints from laboratory experiments
   - Comparison with astrophysical observations

2. Description of specific neutron-star classes
   - Accreted neutron stars
   - Highly-magnetized neutron stars

3. Conclusions & perspectives

Nuclear-energy density functional theory

The nuclear energy density functional theory allows for a consistent description of atomic nuclei (outer crust), inhomogeneous nuclear matter (inner crust) and homogeneous nuclear matter (core).

How to quantify nuclear-matter uncertainties ?

The energy per nucleon of nuclear matter at $T = 0$ around saturation density n_0 and for asymmetry $\eta = (n_n - n_p)/n$, is usually written as

$$e(n,\eta) = e_0(n) + S(n)\eta^2 + o\left(\eta^4\right) \text{ where}$$

$$e_0(n) = a_v + \frac{K_v}{18}\epsilon^2 - \frac{K'}{162}\epsilon^3 + o\left(\epsilon^4\right) \text{ with } \epsilon = (n - n_0)/n_0$$

$$S(n) = J + \frac{L}{3}\epsilon + \frac{K_{sym}}{18}\epsilon^2 + o\left(\epsilon^3\right) \text{ is the } \textbf{symmetry energy}$$

The lack of knowledge is embedded in a_v, K_v, K', etc.

We have developed a family of functionals spanning the range of uncertainties and fitted using the same protocole.

Brussels-Montreal Skyrme functionals (BSk)

For application to extreme astrophysical environments, functionals should reproduce global properties of both finite nuclei and infinite homogeneous nuclear matter.
Chamel et al., Acta Phys. Pol. B46, 349(2015)

Experimental data/constraints:

- $\sim$ 2300 nuclear masses (rms $\sim 0.5 - 0.6$ MeV$/c^2$)
- $\sim$ 900 nuclear charge radii (rms ~ 0.03 fm)
- symmetry energy $29 \leq J \leq 32$ MeV (no good mass fit beyond!)
- incompressibility $K_v = 240 \pm 10$ MeV (giant resonances in nuclei)

Many-body ab initio calculations:

- equation of state of pure neutron matter
- $^1S_0$ pairing gaps in nuclear matter
- effective masses in nuclear matter (+giant resonances in nuclei)
- stability against spin and spin-isospin fluctuations

Phenomenological corrections for atomic nuclei

For atomic nuclei, we add the following corrections to the HFB energy:

- Wigner energy

$$E_W = V_W \exp\left\{ -\lambda\left(\frac{N-Z}{A}\right)^2\right\} + V_W'|N-Z|\exp\left\{-\left(\frac{A}{A_0}\right)^2\right\}$$

$V_W \sim -2$ MeV, $V_W' \sim 1$ MeV, $\lambda \sim 300$ MeV, $A_0 \sim 20$

- rotational and vibrational spurious collective energy

$$E_{\rm coll} = E_{\rm rot}^{\rm crank}\left\{b\ \tanh(c|\beta_2|) + d|\beta_2|\ \exp\{-l(|\beta_2| - \beta_2^0)^2\}\right\}$$

This latter correction was shown to be in good agreement with calculations using 5D collective Hamiltonian.

Goriely, Chamel, Pearson, Phys.Rev.C82,035804(2010)

In this way, these collective effects do not contaminate the parameters (≤ 20) of the functional.

Neutron-matter constraint

BSk22-26 were simultaneously fitted to realistic neutron-matter equations of state in addition to nuclear masses and radii:

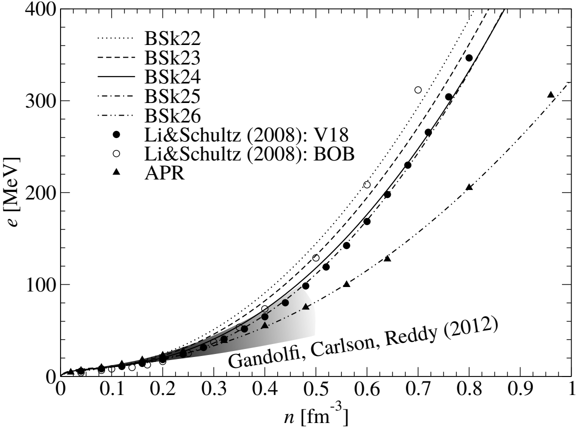

Goriely, Chamel, Pearson, Phys.Rev.C 88, 024308 (2013)

Neutron-matter constraint

BSk22-26 are consistent with more recent neutron-matter calculations based on chiral effective-field theory:

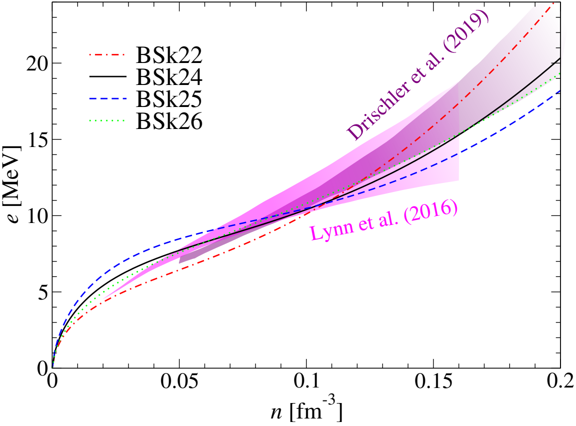

Symmetry-energy constraint

BSk22-26 were adjusted to different values of J. The symmetry energy function $S(n)$ was completely determined by the fit:

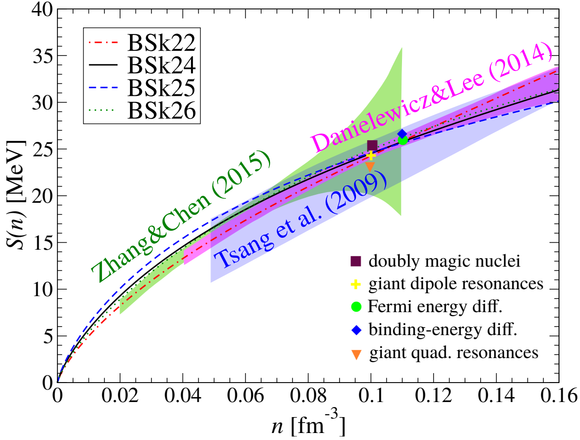

Note that all curves cross at $n \sim (2/3)n_0$ from the atomic mass fit.

Symmetry-energy constraint

BSk22-26 mainly differ in their predictions for the symmetry energy at suprasaturation densities:

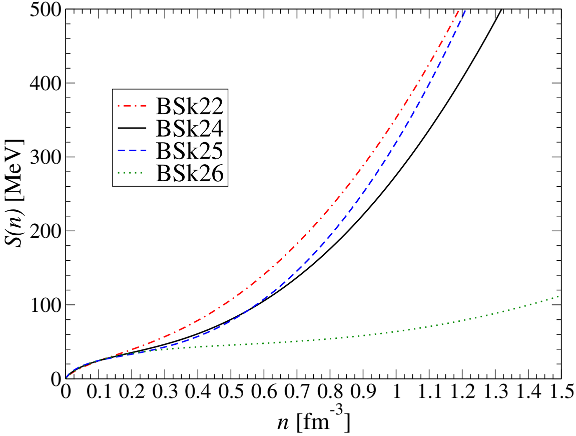

Goriely, Chamel, Pearson, Phys.Rev.C 88, 024308 (2013)

Neutron-star surface

The surface of a neutron star is expected to be made of **iron, the end product of stellar nucleosynthesis** (identification of broad Fe K emission lines from accretion disk around neutron stars in LMXB).

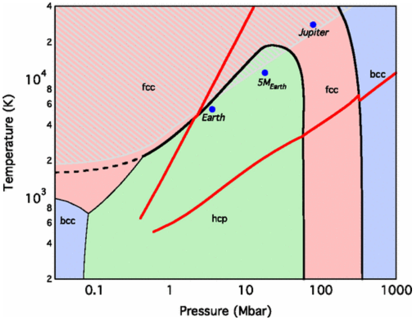

Stixrude, Phys.Rev.Lett. 108, 055505 (2012)

Compressed iron can be studied with **nuclear explosions and laser-driven shock-wave experiments**...

But at pressures corresponding to about **0.1 mm below the surface** (for a star with a mass of $1.4\mathcal{M}_\odot$ and a radius of 12 km) !

Ab initio calculations predict various **structural phase transitions**.

Crystal Coulomb plasma

At a density $\rho_{\rm eip} \approx 2 \times 10^4$ g cm^{-3} (about 22 cm below the surface), the interatomic spacing becomes comparable with the atomic radius.

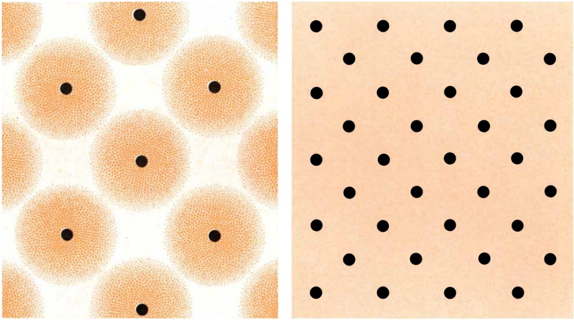

Ruderman, Scientific American 224, 24 (1971)

- At densities $\rho \gg \rho_{\rm eip}$, atoms are crushed into a **dense plasma of nuclei and free electrons**.
- Nuclei become **more neutron rich** with increasing pressure.

Description of the outer crust of a neutron star

Main assumptions:

- cold "catalyzed" matter (full thermodynamic equilibrium)
  Harrison, Wakano and Wheeler, Onzième Conseil de Physique Solvay (Stoops, Brussels, Belgium, 1958) pp 124-146
- pure layers made of nuclei ${}^A_Z\mathrm{X}$
- $\sim$ uniform degenerate electron Fermi gas

  $T < T_{\rm F} \approx 5.93 \times 10^9(\gamma_r - 1)\ \mathrm{K}$

  $$\gamma_r \equiv \sqrt{1 + x_r^2}\,, \qquad x_r \equiv \frac{p_{\rm F}}{m_e c} \approx 1.00884 \left(\frac{\rho_6 Z}{A}\right)^{1/3}$$
- perfect body-centered cubic lattice

  $$T < T_m \approx 1.3 \times 10^5 Z^2 \left(\frac{\rho_6}{A}\right)^{1/3}\ \mathrm{K} \qquad \rho_6 \equiv \rho/10^6\ \mathrm{g\ cm^{-3}}$$

Microscopic inputs: measured atomic masses + deformed Hartree-Fock-Bogoliubov calculations

Pearson et al., MNRAS 481, 2994 (2018)

Analytical determination of the internal constitution

Traditional approach: numerical minimization of the Gibbs free energy per nucleon at different pressures P

Tondeur, A&A 14, 451 (1971); Baym, Pethick, Sutherland, ApJ 170, 299 (1971)

- layers can be easily missed if δP not small enough
- numerically costly (BPS considered 130 even nuclei vs $\sim 10^4$)

New approach: iterative minimization of the pressures between adjacent crustal layers (approximate analytical formulas)

Chamel, Phys. Rev. C 101, 032801(R) (2020)

- very accurate and reliable ($\delta P/P \sim 10^{-3}$ %)
- $\sim 10^6$ times faster
  $\Rightarrow$ well-suited for statistical studies and sensitivity analyses

Freely available computer code:

`http://doi.org/10.5281/zenodo.3719439`

Experimental "determination" of the outer crust

The composition of the crust is completely determined by experimental atomic masses down to about 200m for a $1.4M_{\odot}$ neutron star with a 10 km radius

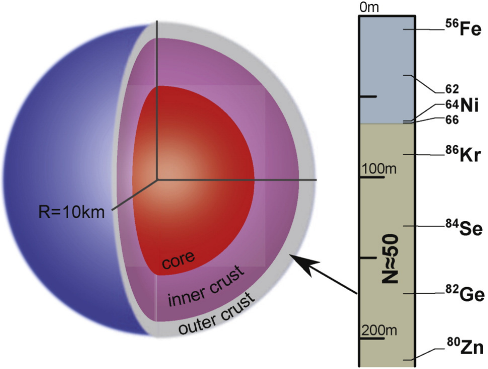

The physics governing the structure of atomic nuclei (magicity) leaves its imprint on the composition.

Due to β equilibrium and electric charge neutrality, Z is more tightly constrained than N: only a few layers with $Z = 28$.

Kreim, Hempel, Lunney, Schaffner-Bielich, Int.J.M.Spec.349-350,63(2013)

Plumbing neutron stars to new depths

Precision mass measurements of ^{82}Zn by the ISOLTRAP collaboration at CERN's ISOLDE radioactive-beam facility in 2013 allowed to "drill" deeper.

Wolf et al.,Phys.Rev.Lett.110,041101(2013)

The composition is very sensitive to uncertainties in nuclear masses. Errors of a few keV$/c^2$ can change the results.

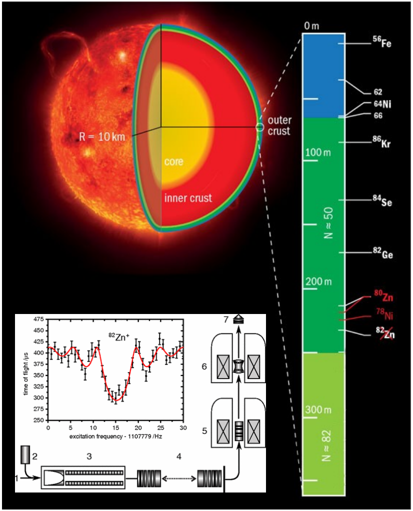

Deeper in the star, recourse must be made to theoretical models.

Role of the symmetry energy on the outer crust

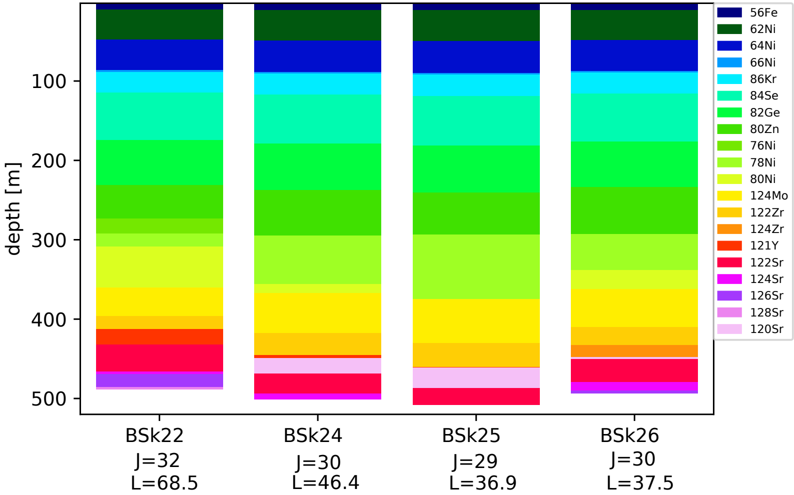

Structure of a neutron star of mass $1.5M_\odot$ and radius 13 km (figure prepared by A. F. Fantina)

Pearson, Chamel, Potekhin, Fantina, Ducoin, Dutta, Goriely MNRAS 481, 2994 (2018)

Role of the symmetry energy on the outer crust

The composition of the outer crust is only slightly influenced by the density dependence of the symmetry energy $S(n)$.

The proton fraction varies roughly as $Y_p = \frac{Z}{A} \sim \frac{1}{2} - \frac{(12\pi^2(\hbar c)^3 P)^{1/4}}{8S}$

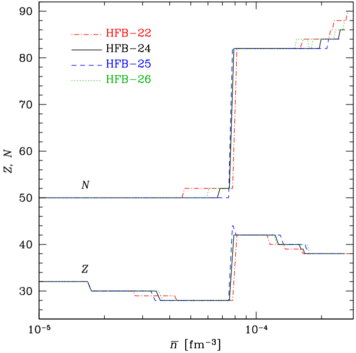

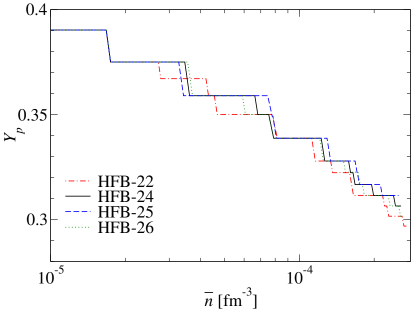

Pearson et al., MNRAS 481, 2994 (2018)

Equation of state of the outer crust

The pressure, determined by electrons, is almost independent of the composition. **Analytical fits**: `http://www.ioffe.ru/astro/NSG/BSk/`

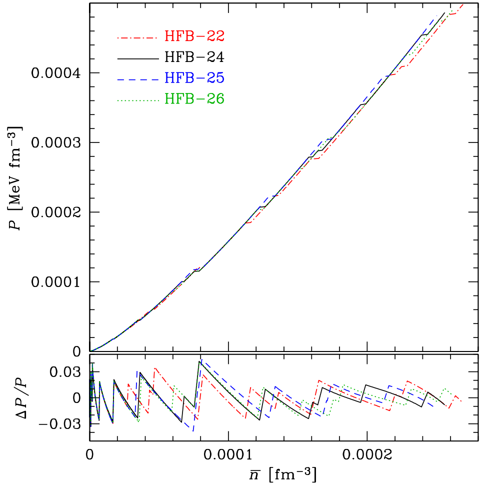

Stratification and equation of state

Transitions between adjacent crustal layers are accompanied by **density discontinuities.**

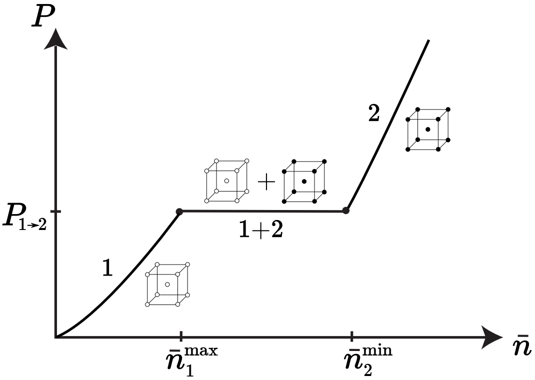

Mixed solid phases cannot exist in a neutron star crust because P has to increase strictly monotonically with $\bar{n}$ (hydrostatic equilibrium).

Compounds in neutron-star crusts?

Multinary ionic compounds made of nuclei with charges $\{Z_i\}$ might exist in the crust of a neutron star.
Dyson, Ann. Phys.63, 1 (1971); Witten, ApJ 188, 615 (1974)

Necessary conditions:

- **stability against weak and strong nuclear processes**.
  Jog&Smith, ApJ 253, 839(1982)
- **stability against the separation into pure (bcc) phases**:

$$\mathcal{R}(\{Z_i/Z_j\}) \equiv \frac{C}{C_{\rm bcc}} f(\{Z_i\}) \frac{\langle Z \rangle}{\langle Z^{5/3} \rangle} > 1$$

where $f(\{Z_i\})$ is the dimensionless lattice structure function of the compound and C the corresponding structure constant.
Chamel & Fantina, Phys. Rev. C94, 065802 (2016)

Stellar vs terrestrial compounds: (i) they are made of nuclei; (ii) electrons form an essentially uniform relativistic Fermi gas.

Some binary and ternary compounds

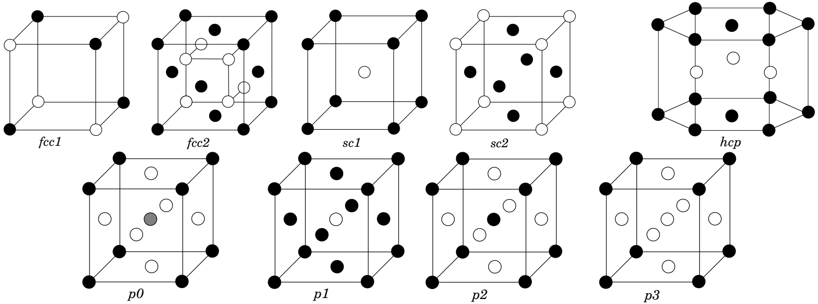

Terrestrial alter ego:

- fcc1: rocksalt (NaCl), oxydes (MgO), carbonitrides (TiN)
- fcc2: fluorite (CaF_2)
- sc1: cesium chloride (CsCl), β-brass (CuZn)
- sc2: auricupride ($AuCu_3$)
- hcp: tungsten carbide (WC)
- p0: perovskite ($BaTiO_3$)

Substitutional compounds in neutron-star crusts

Compounds with CsCl structure are present at interfaces if $Z_1 \neq Z_2$.

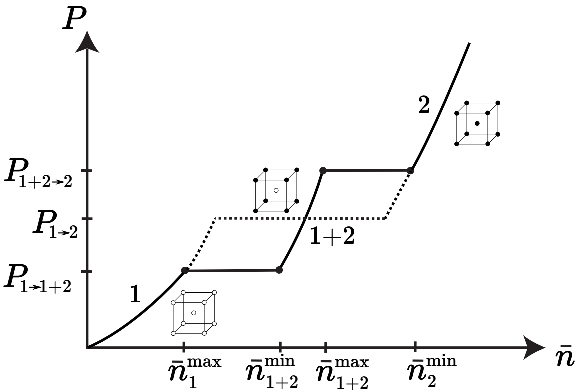

But they only exist over an extremely small range of pressures.

Chamel&Fantina, Phys. Rev. C94, 065802 (2016)

Frozen neutron-star crusts

The composition of the crust may be frozen before or at crystallization due to the quenching of nuclear reactions (results for BSk24):

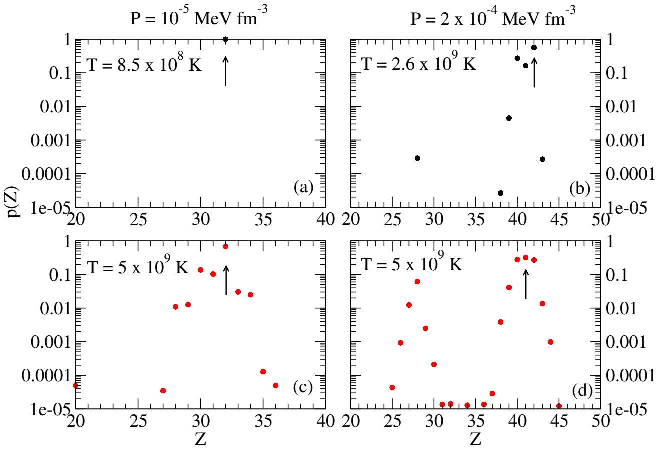

Fantina, De Ridder, Chamel, Gulminelli, A&A 633, A149 (2020)

Frozen neutron-star crusts

Of utmost importance for neutron-star cooling and magnetic-field evolution is the impurity factor $Q_{\rm imp} = \langle (Z - \langle Z \rangle)^2 \rangle$ (results for BSk24):

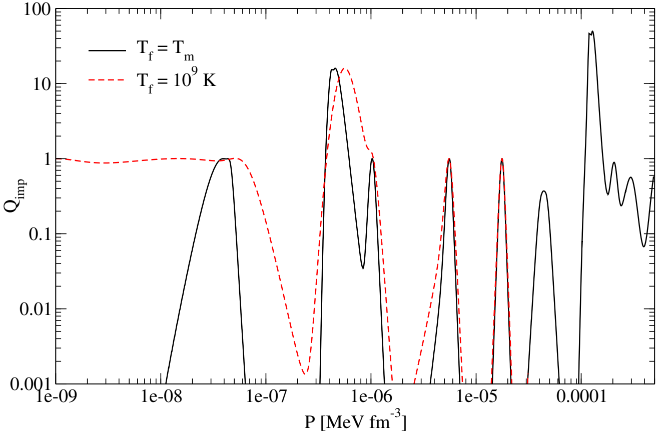

Fantina, De Ridder, Chamel, Gulminelli, A&A 633, A149 (2020)

Description of the inner crust of a neutron star

We use the **4th order Extended Thomas-Fermi+Strutinsky Integral** method with the *same* functional as in the outer crust:

- **semiclassical expansion in powers of $\hbar$**: the energy becomes a functional of $n_n(\boldsymbol{r})$ and $n_p(\boldsymbol{r})$ and their gradients only.
- **proton shell and pairing effects** are added perturbatively (neutron shell effects are negligibly small).

To speed-up the computations, $n_n(\boldsymbol{r}), n_p(\boldsymbol{r})$ are parametrized.

Pearson,Chamel,Pastore,Goriely,Phys.Rev.C91, 018801 (2015)

Pearson,Chamel,Goriely,Ducoin,Phys.Rev.C85,065803(2012)

Onsi,Dutta,Chatri,Goriely,Chamel,Pearson, Phys.Rev.C77,065805 (2008)

- very fast approximation to the full HFB equations
- avoids the pitfalls related to continuum states

Chamel,Naimi,Khan,Margueron,Phys.Rev.C75,055806 (2007)
Margueron&Sandulescu, Neutron Star Crust (Nova, 2012), p. 65
Pastore, Shelley, Baroni, Diget, J. Phys.G44,094003 (2017)

Shelley&Pastore, arXiv:2002.01839

Proton shell effects in stellar environments

The ordinary nuclear shell structure is altered in dense matter:
$Z = 28, 82$ disappear, while $40, 58, 92$ appear (quenched spin-orbit).

Energy per nucleon obtained with BSk24:

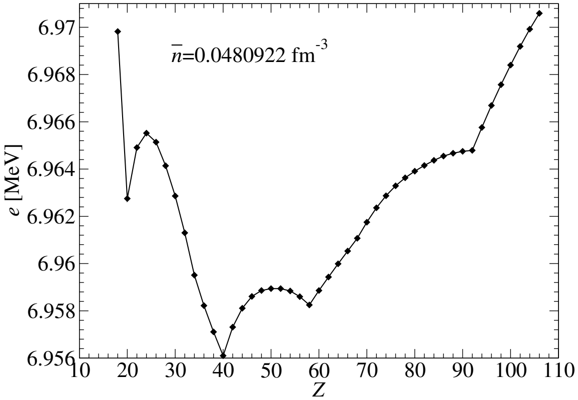

Role of shell effects and symmetry energy

The composition of the inner crust is strongly influenced by the symmetry energy but also by proton shell effects:

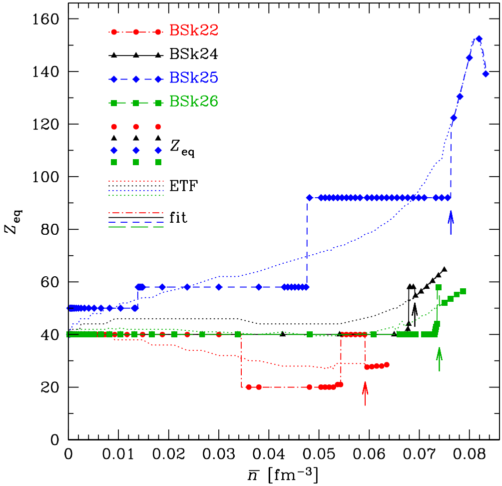

Terrestrial abundances:

Zirconium ($Z = 40$): 0.02%

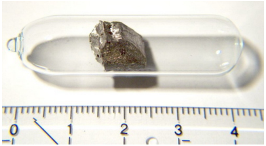

Cerium ($Z = 58$): 0.007%

Symmetry energy and proton fraction

The proton fraction Y_p of the inner crust is governed by the density dependence of the symmetry energy $S(n)$: the lower S the lower Y_p.
Analytical fits: `http://www.ioffe.ru/astro/NSG/BSk/`

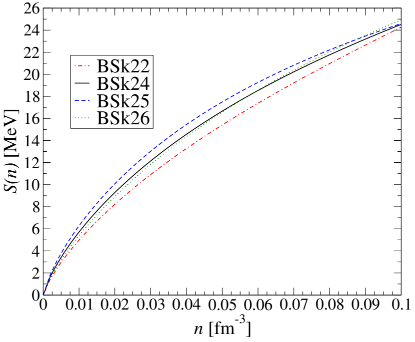

Pearson et al.,MNRAS 481, 2994 (2018)

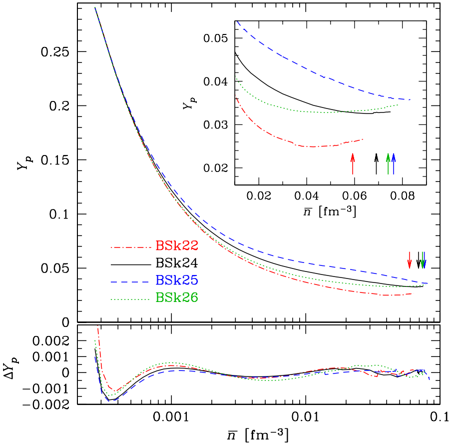

Equation of state of the inner crust

The pressure in the inner crust is related to the slope of the symmetry energy $P \sim n^2 S'(n)$
Analytical fits: `http://www.ioffe.ru/astro/NSG/BSk/`

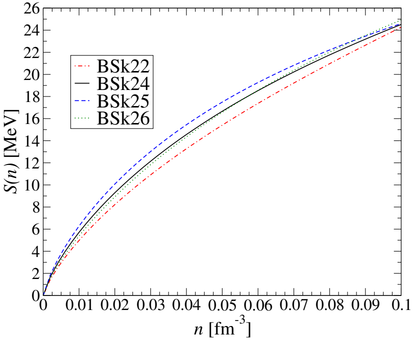

Pearson et al.,MNRAS 481, 2994 (2018)

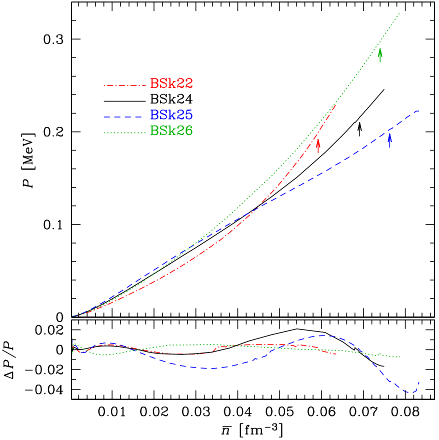

Symmetry energy and proton fraction in the core

The proton fraction Y_p of the core is governed by the density dependence of the symmetry energy $S(n)$: the lower S the lower Y_p.
Analytical fits: `http://www.ioffe.ru/astro/NSG/BSk/`

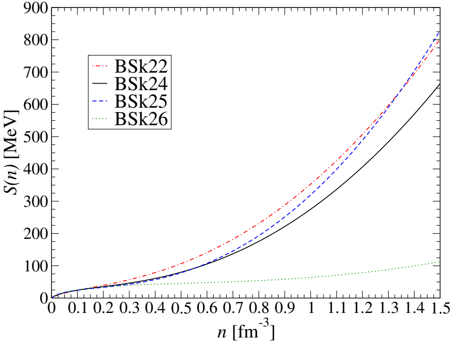

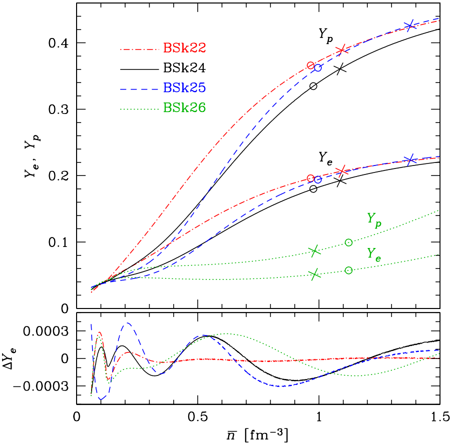

Note that the proton fraction can reach $Y_p \sim 40\%$ in the core.

Symmetry energy and direct Urca

EoS	$n_{\rm DU}$ (fm^{-3})	$\rho_{\rm DU}$ (g cm^{-3})	$M_{\rm DU}/M_\odot$
BSk22	0.333	5.88×10^{14}	1.151
BSk24	0.453	8.25×10^{14}	1.595
BSk25	0.469	8.56×10^{14}	1.612

The direct Urca cooling process is required to explain

- the thermal luminosities of some accreting neutron stars in quiescence (e.g. SAX J1808.4−3658)
- the thermal relaxation of some transiently accreting neutron stars (e.g. MXB 1659−29).

- The dUrca process is allowed in all models but BSk26.
- The low value for $M_{\rm DU}$ predicted by BSk22 implies that dUrca would operate in most neutron stars, at variance with observations.

Nuclear pasta mantle

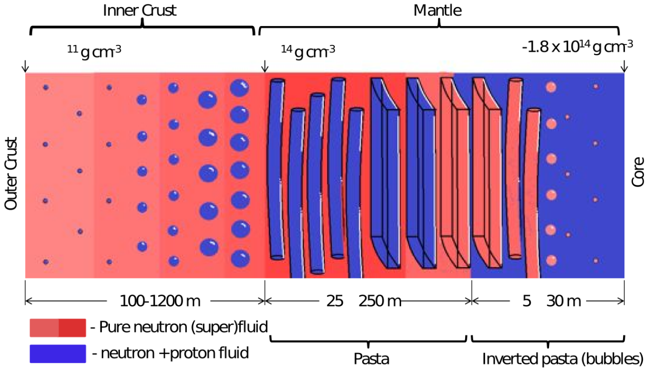

picture from W. G. Newton

- Pastas form for filling fraction $> 1/8$ (liquid drop model)
- The shapes depend on symmetry energy and shell effects
- The equation of state is insensitive to pastas.

Pearson et al., Phys. Rev. C 101, 015802 (2020); Kubushishi's master thesis (2020)

Adiabatic index and polytropic approximation

Unified equations of state can hardly be parametrized by polytropes!

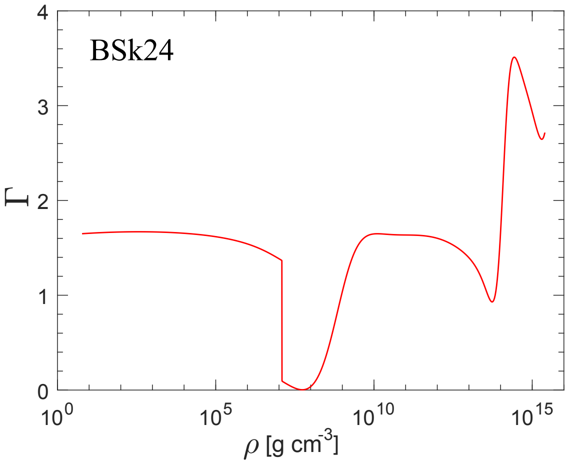

Gross properties of neutron stars

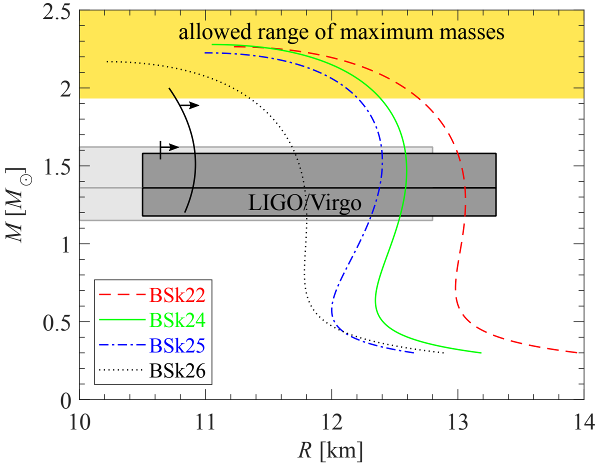

Perot,Chamel,Sourie,Phys.Rev.C 100, 035801 (2019)

Stiff symmetry energy (BSk22) is marginally compatible with LIGO-Virgo constraints on NS radii from GW170817.

Tidal deformability of neutron stars

The tidal deformability coefficient Λ of a $1.4M_{\odot}$ neutron star is strongly correlated with R hence also with the symmetry energy:

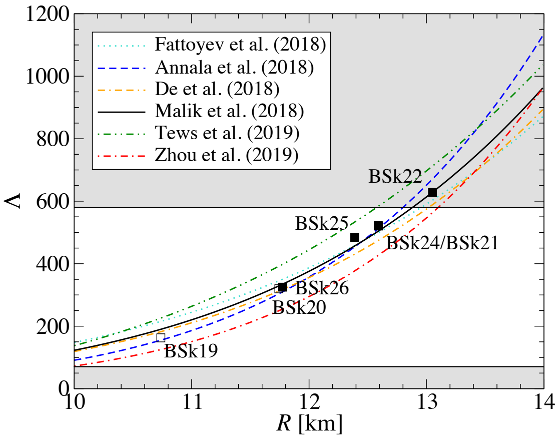

Perot,Chamel,Sourie,Phys.Rev.C 100, 035801 (2019)

Symmetry energy and Love number

The Love number k_2 is insensitive to the symmetry energy:

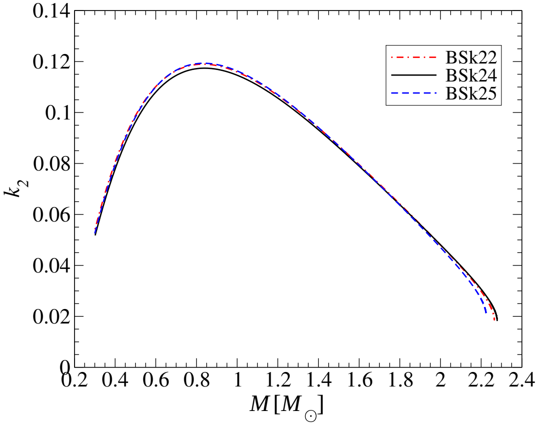

Perot,Chamel,Sourie,Phys.Rev.C 100, 035801 (2019)

The dependence of $\Lambda = (2/3)k_2(Rc^2/GM)^5$ on the symmetry energy thus arises mainly from the factor R^5.

Symmetry energy and Love number

The Love number is mostly governed by the neutron-matter stiffness:
(BSk19 softest, BSk24 stiffest)

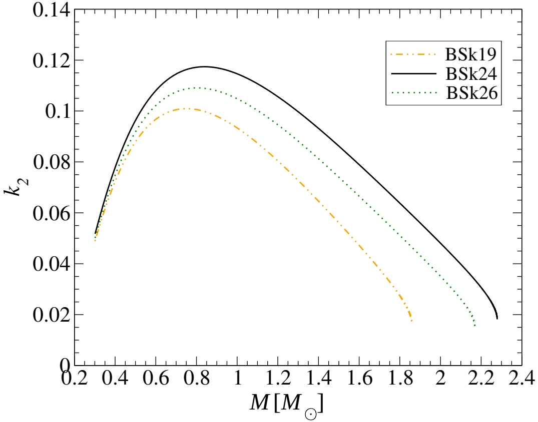

Perot,Chamel,Sourie,Phys.Rev.C 100, 035801 (2019)

Role of the crust on the tidal deformability

Comparison with purely homogeneous neutron stars for BSk24:

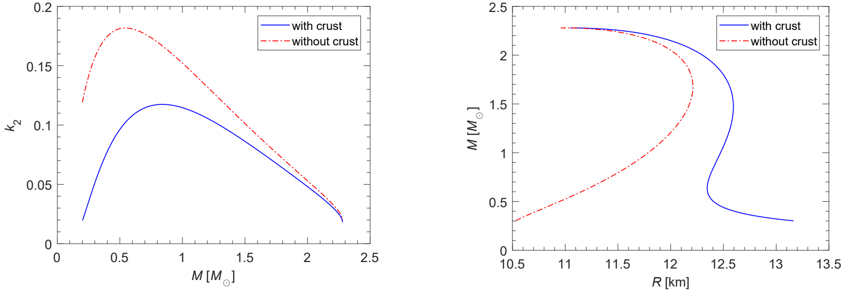

- Changes in k_2 are essentially due to changes in R
- Analytic formula for k_2 from EoS of homogeneous matter only

Changes in $\Lambda \propto k_2 R^5$ are small ($< 1\%$): the strong reduction of k_2 is mitigated by the increase of R.

Perot,Chamel,Sourie,Phys.Rev.C 101, 015806 (2020)

Accretion and X-ray binaries

The composition of the surface layers may be changed by

- the **fallback** of material from the supernova explosion,
- the **accretion** of matter from a stellar companion.

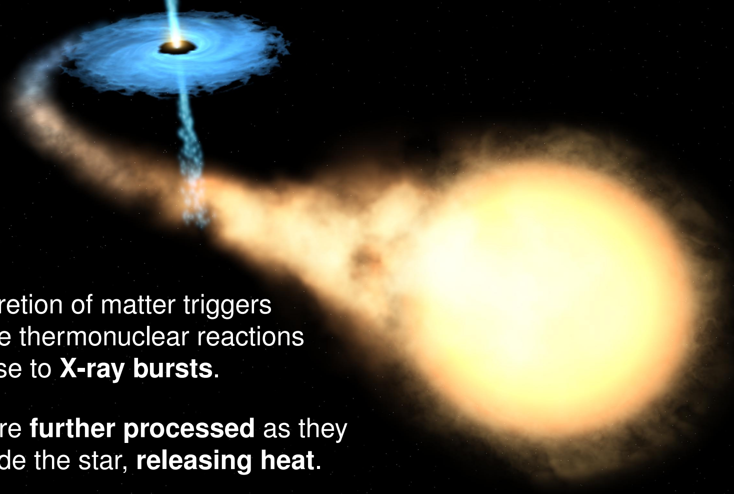

The accretion of matter triggers explosive thermonuclear reactions giving rise to **X-ray bursts.**

Ashes are **further processed** as they sink inside the star, **releasing heat.**

Compounds in accreted crusts

Various compounds can form from ashes of X-ray bursts:

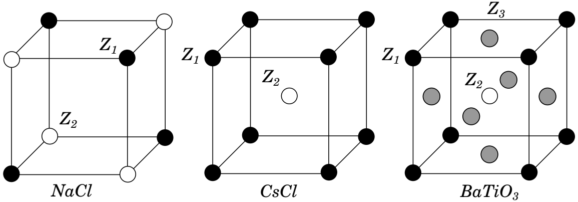

- Rocksalt: **AgNe**.
- Cesium chloride: **AgCa**, AgTi, AgCr, AgFe, **AgCo**, AgNi, AgZn, AgGe, AgAs, AgSe, **AgKr**, **KrCa**, KrTi, KrCr, KrFe, **KrCo**, KrNi, KrZn, KrGe, KrAs, KrSe, SeCa, SeTi, SeCr, SeFe, SeCo, SeNi, SeZn, SeGe, SeAs, AsCa, AsTi, AsCr, AsFe, AsCo, AsNi, AsZn, AsGe, GeCa, GeTi, GeCr, GeFe, GeCo, GeNi, GeZn, ZnCa, ZnTi, ZnCr, ZnFe, ZnCo, ZnNi, NiCa, NiTi, NiCr, NiFe, NiCo, **CoCa**, CoTi, CoCr, CoFe, FeCa, FeTi, FeCr, CrCa, **CrTi**, TiCa.
- Perovskite: $AgNeO_3$.

Chamel, J. Phys. Conf.S.932, 012039 (2017)

Composition of accreted crusts and heating

The original crust is buried in the core and replaced by accreted material with very different properties.

Composition and crustal heating for ashes made of ^{56}Fe:

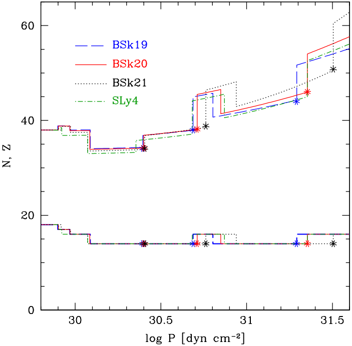

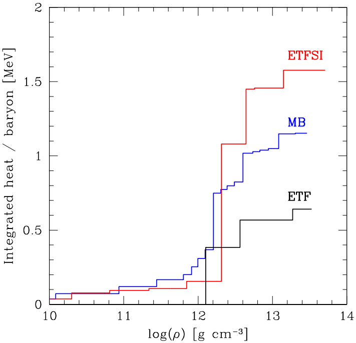

Results are very sensitive to shell effects (magic number $Z = 14$)

Fantina,Zdunik,Chamel,Pearson,Haensel,Goriely, A&A 620, A105 (2018)

Highly-magnetized neutron stars

Some neutron stars are endowed with **extremely high surface magnetic fields** $\sim 10^{14} - 10^{15}$ G, as inferred from spin-down and spectroscopic studies.

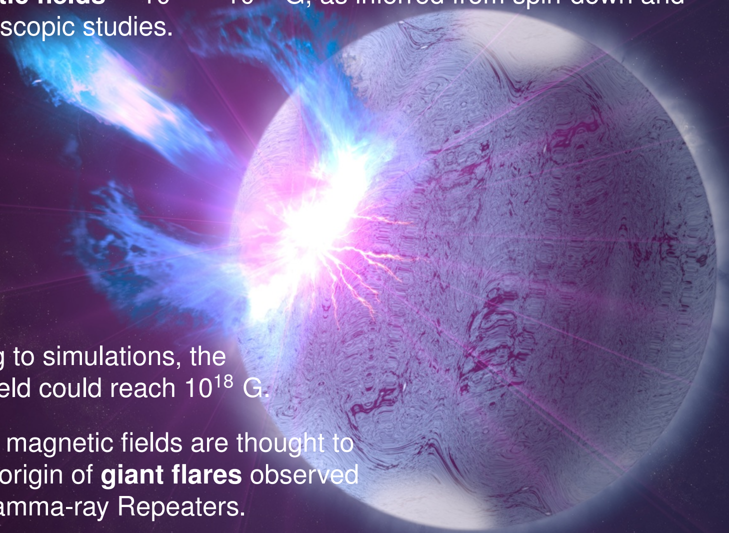

According to simulations, the internal field could reach 10^{18} G.

Very high magnetic fields are thought to be at the origin of **giant flares** observed in Soft Gamma-ray Repeaters.

Role of a high magnetic field on dense matter?

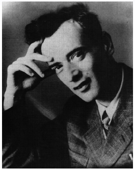

At the surface of neutron stars $B \lesssim 2 \times 10^{15}$ G.

The electron motion perpendicular to $\boldsymbol{B}$ is quantised into **Landau orbitals** with a characteristic scale $a_m = a_0\sqrt{B_{\rm at}/B}$, where a_0 is the Bohr radius

For $B \gg B_{\rm at} = m_e^2 e^3 c/\hbar^3 \simeq 2.35 \times 10^9$ G, atoms are expected to adopt a very elongated shape along $\boldsymbol{B}$ and to form **linear chains**
Ruderman, PRL27, 1306 (1971); Medin&Lai, Phys.Rev. A74, 062508 (2006)

The attractive interaction between these chains could lead to a transition into a **condensed phase** with a surface density

$$\rho_s \sim 560 A Z^{-3/5} (B/10^{12}\ \mathrm{G})^{6/5}\ \mathrm{g\ cm^{-3}}$$

In deeper regions of the crust, matter is **very stiff**

$$\rho \approx \rho_s \left(1 + \sqrt{\frac{P}{P_0}}\right) , \quad P_0 \simeq 1.45 \times 10^{20} (B/10^{12}\ \mathrm{G})^{7/5} \left(\frac{Z}{A}\right)^2 \mathrm{dyn\,cm^{-2}}$$

Lai, Rev.Mod.Phys.73, 629 (2001); Chamel et al., Phys.Rev.C86, 055804 (2012)

The intriguing case of RX J1856.5-3754

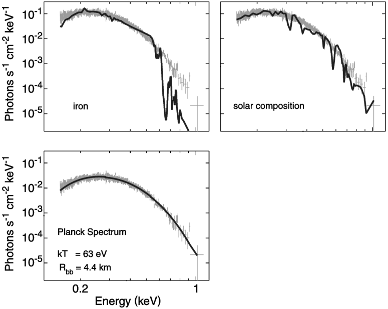

Fig. 3: The Chandra LETG X-ray spectrum of RX J1856 fitted with (non-magnetic) photospheric models assuming pure iron and solar composition. The best fit is obtained with a Planck spectrum (Burwitz et al. 2003).

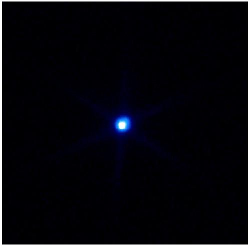

X-ray observations with Chandra

Turolla et al., ApJ 603, 265 (2004)
van Adelsberg et al., ApJ 628, 902 (2005)
Trümper (2005), astro-ph/0502457

Recent review: *Potekhin et al., Space Sci. Rev. 191, 171 (2015)*

The thermal X-ray emission is best fitted by a **black body** spectrum: evidence for a condensed surface? The presence of high ***B*** has found additional support from recent optical polarimetry measurements.
Mignani et al., MNRAS 465, 492 (2017)

Composition of highly-magnetized crust

The composition changes with B, but not the structure (bcc).

Kozhberov, Astrophys. Space Sci.361, 256 (2016)

Equilibrium nuclides for HFB-24 and $B_\star \equiv B/(4.4 \times 10^{13}$ G):

Nuclide	$B_\star$
^{58}Fe(-)	9
^{66}Ni(-)	67
^{88}Sr(+)	859
^{126}Ru(+)	1031
^{80}Ni(-)	1075
^{128}Pd(+)	1445
^{78}Ni(-)	1610
^{79}Cu(-)	1617
^{64}Ni(-)	1668
^{130}Cd(+)	1697
^{132}Sn(+)	1989

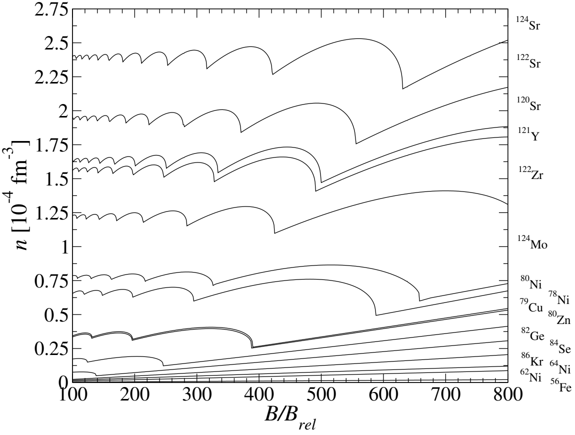

Quantum oscillations

The neutron-drip density exhibits typical **quantum oscillations**.

Example using HFB-24:

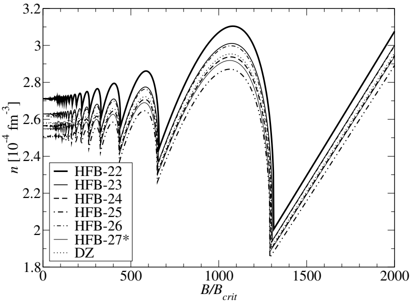

Universal oscillations:

$$\frac{\bar{n}_{\rm drip}^{\rm min}}{\bar{n}_{\rm drip}(B_\star=0)} \approx \frac{3}{4}$$

$$\frac{\bar{n}_{\rm drip}^{\rm max}}{\bar{n}_{\rm drip}(B_\star=0)} \approx \frac{35+13\sqrt{13}}{72}$$

In the strongly quantising regime,

$$\bar{n}_{\rm drip} \approx \frac{A}{Z}\frac{\mu_e^{\rm drip}}{m_e c^2}\frac{B_\star}{2\pi^2\lambda_e^3}\left[1-\frac{4}{3}C\alpha Z^{2/3}\left(\frac{B_\star}{2\pi^2}\right)^{1/3}\left(\frac{m_e c^2}{\mu_e^{\rm drip}}\right)^{2/3}\right]$$

Chamel et al.,Phys.Rev.C91, 065801(2015); J.Phys.:Conf.Ser.724, 012034 (2016)

Quantum oscillations

The neutron-drip density exhibits typical **quantum oscillations**.

Example using HFB-24:

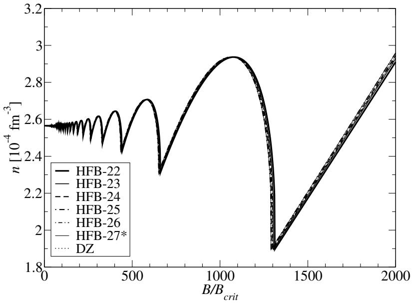

Universal oscillations:

$$\frac{\bar{n}_{\rm drip}^{\rm min}}{\bar{n}_{\rm drip}(B_\star=0)} \approx \frac{3}{4}$$

$$\frac{\bar{n}_{\rm drip}^{\rm max}}{\bar{n}_{\rm drip}(B_\star=0)} \approx \frac{35+13\sqrt{13}}{72}$$

In the strongly quantising regime,

$$\bar{n}_{\rm drip} \approx \frac{A}{Z}\frac{\mu_e^{\rm drip}}{m_e c^2}\frac{B_\star}{2\pi^2\lambda_e^3}\left[1-\frac{4}{3}C\alpha Z^{2/3}\left(\frac{B_\star}{2\pi^2}\right)^{1/3}\left(\frac{m_e c^2}{\mu_e^{\rm drip}}\right)^{2/3}\right]$$

Chamel et al.,Phys.Rev.C91, 065801(2015); J.Phys.:Conf.Ser.724, 012034 (2016)

Analytical determination of the internal constitution

Traditional approach: numerical minimization of the Gibbs free energy per nucleon at different pressures P

Lai&Shapiro, ApJ 383, 745 (1991)

- layers can be easily missed if δP not small enough
- numerically costly (calculations for a range of B)

New approach: iterative minimization of the pressures between adjacent crustal layers (approximate analytical formulas)

Chamel, Phys. Rev. C, in press

- very accurate ($\delta P/P \sim 0.1\%$)
- $\sim 10^4$ times faster
  $\Rightarrow$ well-suited for statistical studies and sensitivity analyses

Freely available computer code:

`http://doi.org/10.5281/zenodo.3839787`

Unified treatment of magnetar crusts

Landau-Rabi quantization of electron motion changes also the composition and the equation of state of the inner crust.

Results obtained with BSk24:

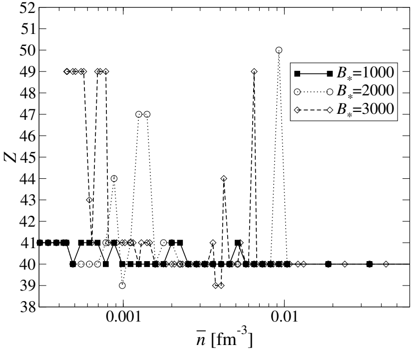

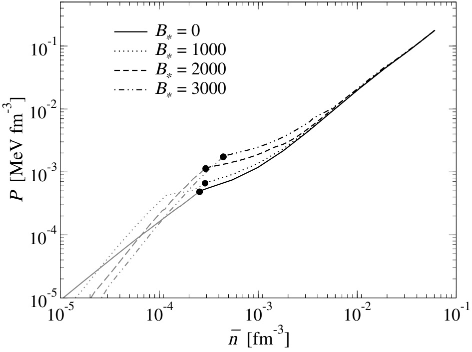

Mutafchieva, Chamel, Stoyanov, Pearson, Mihailov, Phys. Rev. C 99, 055805 (2019)

Conclusions & Perspectives

We have constructed **unified and thermodynamically consistent equations of state for NS** based on **precision-fitted nuclear functionals** varying the neutron-matter stiffness & symmetry energy.

Analytical fits: `http://www.ioffe.ru/astro/NSG/BSk/`

- The inner crust (core) composition is very sensitive to the symmetry energy at densities below (above) saturation.
- Stiffer symmetry energy leads to larger NS radii.
- The symmetry energy has essentially no impact on k_2.
- Λ depends on symmetry energy through R.
- Stiff symmetry energy disfavored by GW170817.
- Very soft and stiff symmetry energies ruled out by NS cooling.

Our long-term objective is to provide **consistent microscopic inputs** for modeling the dynamics of compact stars.

Nuclear-matter parameters

	BSk22	BSk23	BSk24	BSk25	BSk26
a_v [MeV]	-16.088	-16.068	-16.048	-16.032	-16.064
n_0 [fm^{-3}]	0.1578	0.1578	0.1578	0.1587	0.1589
J [MeV]	32.0	31.0	30.0	29.0	30.0
L [MeV]	68.5	57.8	46.4	36.9	37.5
K_{sym}[MeV]	13.0	-11.3	-37.6	-28.5	-135.6
K_v [MeV]	245.9	245.7	245.5	236.0	240.8
K' [MeV]	275.5	275.0	274.5	316.5	282.9
M_s^*/M	0.80	0.80	0.80	0.80	0.80
M_v^*/M	0.71	0.71	0.71	0.74	0.65

Lower and higher values of J were considered but yielded substantially worse fits to atomic masses.

Goriely, Chamel, Pearson, Phys.Rev.C 88, 024308 (2013).